Int. J. Multiphase Flow Vol. 6, pp. 329–344
Pergamon/Elsevier, 1980. Printed in Great Britain

STEAM CHUGGING IN A BOILING WATER REACTOR PRESSURE-SUPPRESSION SYSTEM

J. H. PITTS†

Gesellschaft für Reaktorsicherheit (GRS) mbH, 8046 Garching, Federal Republic of Germany

(*Received* 24 *July* 1979; *in revised form* 4 *January* 1980)

Abstract—Results of a transient analysis predicting the general characteristics of steam chugging compare well with the results of two large scale experiments: GKM II, test 21 and GKSS, test 16. Predicted fundamental periods of chugging are within 5 and 16 per cent of the respective experimental values. The results of the analysis include effects of air in the drywell, momentum loss and heat transfer in the condensation pipe, direct contact condensation heat transfer at the gas–water interface and momentum and heat transfer in the wetwell water pool. Bubble shape is calculated in two-dimensional cylindrical coordinates.

Required inputs to the analysis include the geometry, initial conditions and constants to determine both the steam inlet mass flowrate to the drywell as a function of time and conduction heat transfer through the wall of the condensation pipe. There are no arbitrary free parameters which must be specified to predict specific experiments. Rather, the analysis is based on fundamental physical phenomena, experimental coefficients documented for general heat transfer and fluid mechanics characteristics and standard analytical techniques.

The random nature of steam chugging observed in some experiments is partially explained by predicted regimes of chugging and changes in the maximum extent of a bubble below the condensation pipe exit during each regime.

INTRODUCTION

The basic design of Boiling Water Reactor (BWR) power plants includes a pressure–suppression system which is built to keep the pressure inside the containment shell below allowable bounds in case of an accident. The most restrictive design conditions conceived for a BWR pressure–suppression system occur during a postulated loss-of-coolant accident (LOCA). This paper concerns one phenomenon called "steam chugging" which could occur during late stages of a LOCA and which could produce large forces on components in a BWR pressure–suppression system.

Steam chugging can be explained by examining the schematic diagram of the typical BWR pressure–suppression system shown in figure 1. This particular figure shows the Kraftwerk Union Model 69‡ system. Other systems may differ in design, but they all contain basically the same components and function in a similar fashion. The Model 69 pressure–suppression system consists of (1) a drywell initially filled with air at about ambient pressure; (2) a wetwell which is approximately half-filled with water and half-filled with air, again at about ambient pressure; and (3) a minimum of 58 vertical condensation pipes 0.6 m in diameter that connect the drywell to the wetwell. The bottoms of the condensation pipes are open and are submerged below the water surface. The outsides of the drywell and wetwell form the containment shell. The reactor pressure vessel, as well as the reactor, are located inside the drywell.

During a postulated large break LOCA, a steam line or a water recirculation line is assumed to break near the reactor pressure vessel. Steam or water or both are discharged into the drywell at a maximum conceivable flowrate; pressure into the drywell increases. During the first 1/4 s or so water, initially in the condensation pipes, is forced into the wet well water pool. Then air,

†This work was completed while the author was on a Professional Research Leave from the Lawrence Livermore Laboratory, Livermore, CA 94550, U.S.A.

‡Reference to a company or product name does not imply approval or recommendation of the product by the University of California or the U.S. Dept. of Energy to the exclusion of others that may be suitable.

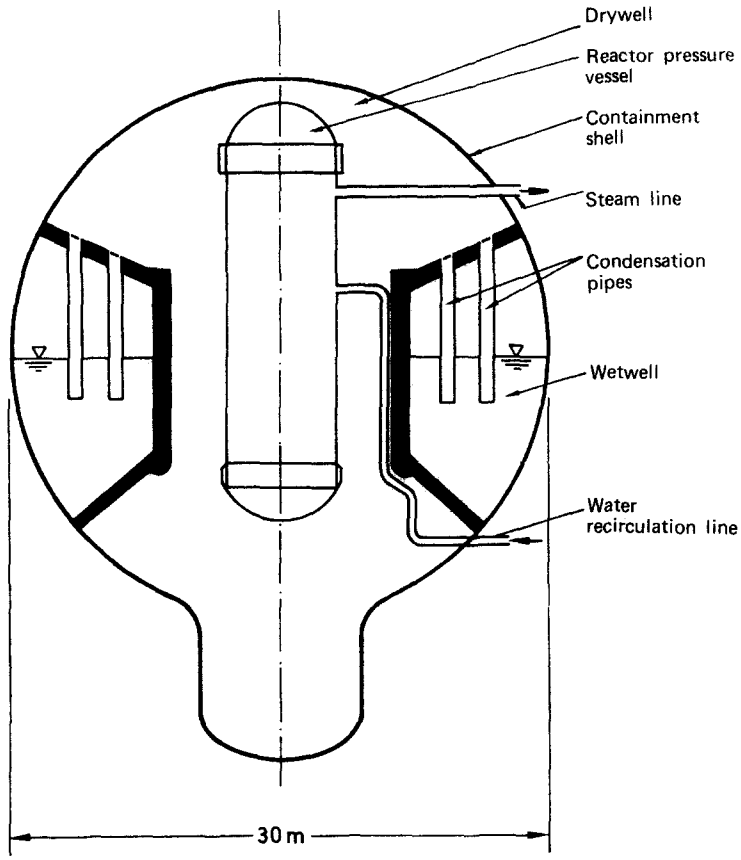

Figure 1. Schematic of the Kraftwerk Union (KWU) model 69 Boiling Water Reactor (BWR) pressure-suppression system.

followed by steam, is discharged into the wetwell. Air bubbles float to the top of the wetwell and the steam condenses as it mixes with the water.

Water motion inside the wetwell is vigorous during the first few minutes, but it gradually reduces in magnitude as the steam discharged into the drywell decreases. Discharge of fluid into the drywell is continuous during all the stages of a LOCA. Initally the discharge of fluid through the condensation pipes into the wetwell is continuous, but after a few minutes, when the flowrate is small and most of the air has been purged from the drywell, the discharge through the condensation pipes can become oscillatory. Oscillations were first observed during the Marviken experiments in Sweden, and later in tests documented by Koch & Karwat (1976) and Aust *et al.* (1977). In these tests, water actually entered the condensation pipe during part of the oscillatory cycle. The water hit the condensation pipe wall and produced a loud, low frequency sound which gave rise to the name "steam chugging".

Steam chugging occurs because of large changes in the condensation rate. As steam is discharged into the water pool and a steam bubble is formed, the condensation rate increases. At times later than a few minutes after the start of the LOCA, this condensation rate can exceed the steam mass flowrate into the drywell, so that the driving pressure in the drywell decreases and water flows back into the condensation pipes. The condensation rate then decreases, the driving pressure builds up, and water is forced back out of the pipes. Steam is discharged into the water pool again and the process repeats.

Large forces generated during the steam chugging process result from a rapid decrease in momentum which occurs when steam bubbles collapse and water motion stops suddenly. The magnitudes of these forces are of interest to designers of reactor containment structures and to those involved in licencing procedures.

Class (1977) examined the general phenomena of pressure oscillations when steam is flowing through the condensation pipes. His analysis is complex and requires specification of a number of unknown input parameters (free parameters). These unknown input parameters must be selected carefully, using prior knowledge of the specific problem, in order to obtain satisfactory results. In spite of this difficulty, his analysis was the first documented attempt to predict steam chugging, and his work gave valuable insight into the phenomena.

Kowalchuk & Sonin (1978) developed an analysis for steam chugging to explore the effects of operational input parameters on the gross motion of the fluids and to determine how the process scales between a model and prototype. They recognized, as we did, that the major uncertainty in the phenomena was the mechanism for direct contact condensation heat transfer between steam and water. Their method of determining a limiting rate of condensation using turbulent diffusion of heat into the water adjacent to the interface was incorporated into the present work. Their analysis was not intended for design calculations or predictions and, indeed, there was divergence when their results were compared to those available from large scale experiments.

Sargis *et al.* (1979) developed an analysis to investigate the phenomenology of steam chugging. Their analysis includes prediction of wall pressures, but again requires specification of several unknown input parameters. Results are in reasonable agreement with small scale experiments performed at SRI and documented by Andeen & Marks (1979). Prediction of a large scale test has been initiated, but results are not yet available.

Chan *et al.* (1978) conducted tests on a small scale (38 mm inside diameter pipe) and established flow regimes for steam chugging. These flow regimes depended mainly upon the water pool subcooling and the steam mass flux. They expect that other parameters may shift boundaries between the various flow regimes, but that the physics of each regime should remain the same. There is difficulty, however, in quantitatively scaling their results to prototype size systems.

The present work includes: (1) a transient analysis of the steam chugging phenomena; (2) results that show the dependency on major parameters and offer insight into the complex mechanisms involved in steam chugging; and (3) two large scale test predictions that are in agreement with available experimental data. The analysis may be used to predict general characteristics of steam chugging in nuclear power plants or experimental tests, can be incorporated into larger general computer programs, or can be used as part of a BWR pressure–suppression system fluid-structure analysis.

ANALYTICAL DEVELOPMENT

The complexity of the steam chugging phenomena prevents completion of an analysis which predicts exact spatial and temporal variation of fluid motion. The approach taken here was to simplify the problem and then use proven analytical techniques to obtain general characteristics of steam chugging. It can be argued that until uncertainties in the basic mechanisms can be reduced, particularly the uncertainty of direct contact condensation heat transfer between steam and water, inclusion of more detailed physics in the analysis would offer little additional insight. In addition, the general characteristics are more important than the detailed fluid motions to designers of power plant equipment. The general characteristics are used to find the maximum stresses, deflections, etc. which determine the operating limits to be observed. The exact fluid motion would need to be averaged over space and time before it could be utilized by reactor designers.

As shown in figure 2, our model includes a drywell, a single vertical condensation pipe, and a wetwell. Steam mass flowrate into the drywell, $\dot{m}_i$, must be specified from experimental data or analytical predictions. Although any reasonable mathematical function can be utilized, a

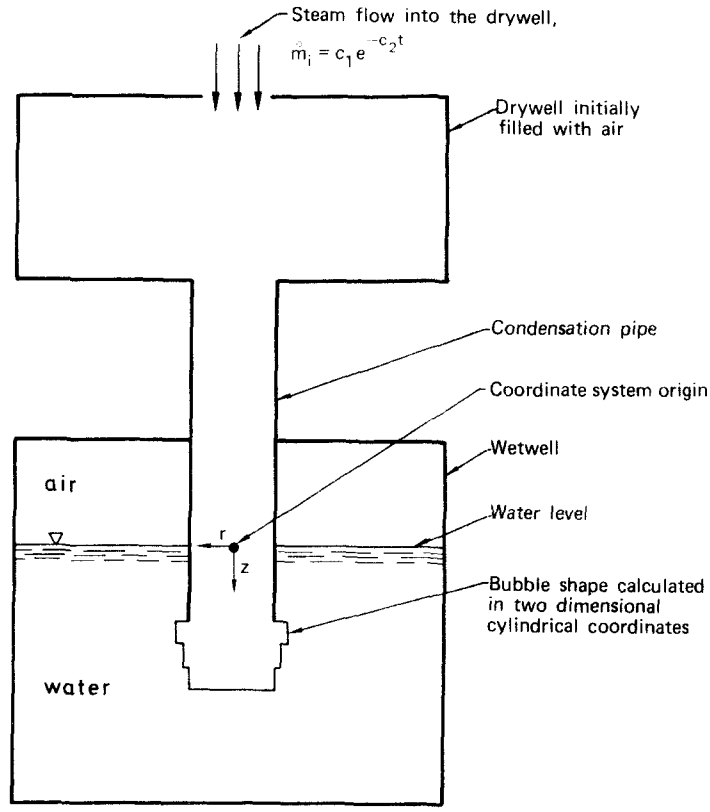

Figure 2. Analytical model which is used to predict general characteristics of steam chugging.

negative exponential with time

$$\dot{m}_i = c_1 e^{-c_2 t}, \qquad [1]$$

is representative of expected conditions. In [1], $\dot{m}_i$ is the inlet saturated steam mass flowrate into the drywell, c_1 and c_2 are constants, and t is time. Mass is conserved in the drywell so that the drywell pressure is a function of time. Drywell temperature is taken to be that of saturated steam at the pressure present.

The only other fluid in the drywell is air. If the air in the drywell is considered to mix instantaneously with the steam, the variation of total mass of fluid (steam plus air) in the drywell is assumed to be small, condensation is neglected, and a perfect gas approximation is utilized,† then

$$\frac{dm}{dt} + p(t)m = q(t), \qquad [2]$$

where

$$p(t) = \frac{c_1}{m_T} e^{-c_2 t}, \qquad [3]$$

†A more realistic approach to mixing in the drywell would need to include geometrical effects and as yet unmeasured experimental values. Inclusion of these geometrical effects is complex and of minor importance when compared to the uncertainty in direct contact condensation heat transfer needed to precisely determine the fluid motion in the wetwell. Similarly, both the actual variation of fluid mass (<25 per cent) and fraction of steam condensed (<10 per cent) in the drywell produce small effects. The perfect gas approximation is reasonable because the pressure varies only from 0.1 to 0.3 MPa.

$$q(t) = \mathring{m}_i \,. \qquad [4]$$

Here m is the mass of steam and m_T is the total mass of fluid in the drywell. Equation [2] is solved for m which allows the mass fraction of air in the drywell, χ_a, to be determined as follows:

$$\chi_a = e^{(c_1/c_2 m_T)}(e^{-c_2 t} - 1). \qquad [5]$$

Pressure loss in the condensation pipe between the drywell and the gas–water interface is calculated by assuming steady incompressible flow.† This pressure loss is greater or less than zero depending on the direction of the mass flowrate through the condensation pipe. The mass flowrate is set equal to the sum of the steam condensation rate in the condensation pipe and wetwell plus the rate at which gas must be added or subtraced to maintain pressure compatibility as the gas volume changes in the condensation pipe and bubble.

Fluid motion of the water and the growth or collapse of a bubble are calculated in two-dimensional cylindrical coordinates. Only axial motion is permitted inside the condensation pipe. A control volume of water, consisting of a cylinder which has a diameter equal to that of the condensation pipe, is formed (see figure 3a). The length is equal to the distance from the gas–water interface to the end of the condensation pipe plus one pipe diameter. The length of the control volume outside the pipe is held constant and acts as a virtual mass. When there is no water inside the pipe, the control volume consists of only the virtual mass. This length of virtual mass is standard in many fluid dynamic solutions.

An integral form of the momentum equation is used to determine acceleration of the water (Shames 1962). In the axial direction, the following equation is used:

$$F_z + \int_{\text{C.V.}}\int\int B_z \rho \, \mathrm{d}v = \int_{\text{C.S.}}\int V_z(\rho V_z \cdot \mathrm{d}A) + \frac{\partial}{\partial t}\int_{\text{C.V.}}\int\int V_z(\rho \, \mathrm{d}v) \,, \qquad [6]$$

where F_z represents the surface forces acting in the vertical direction; B_z is a vertical body force per unit mass (gravity); $\mathrm{d}v$ is a differential volume; V_z is the component of fluid velocity in the vertical direction; ρ is density; and $\mathrm{d}A$ is a differential control surface. Equation [6] contains no "r" direction terms and is applied to the control volumes for the axial momentum equation shown in figure 3. This implies that the fluid motion in these control volumes is essentially axial, which is necessarily correct for the portion of the control volume in figure 3(a) that is inside the condensation pipe. Utilization of this assumption for the portion of the control volume in figure 3(a) outside the condensation pipe and for the axial momentum equation control volume in figure 3(b) is justified because: (1) fluid leaving the condensation pipe must have essentially an axial motion; (2) high speed motion pictures of large scale experiments show that the bubbles grow in basically a cylindrical form; and (3) results for both relatively large and relatively small steam mass flowrates through the condensation pipe generated with this assumption, shown later, agree with experimental data.

This assumption is not valid during bubble collapse when large instabilities (e.g. Taylor instabilities) occur. These instabilities become dominant during the period of bubble collapse and act to increase the surface area available for heat transfer. Unfortunately, inclusion of the motion caused by these instabilities makes the problem so complex that solution with available computers becomes impractical. The procedure outlined here, however, gives a good approximation of the bubble shape during the periods of bubble growth and start of bubble collapse. Only in the later

†The assumption of incompressible flow is within 15 per cent and in most cases within 5 per cent of a more accurate compressible flow calculation. The simpler incompressible flow assumption is considered to be adequate for this study.

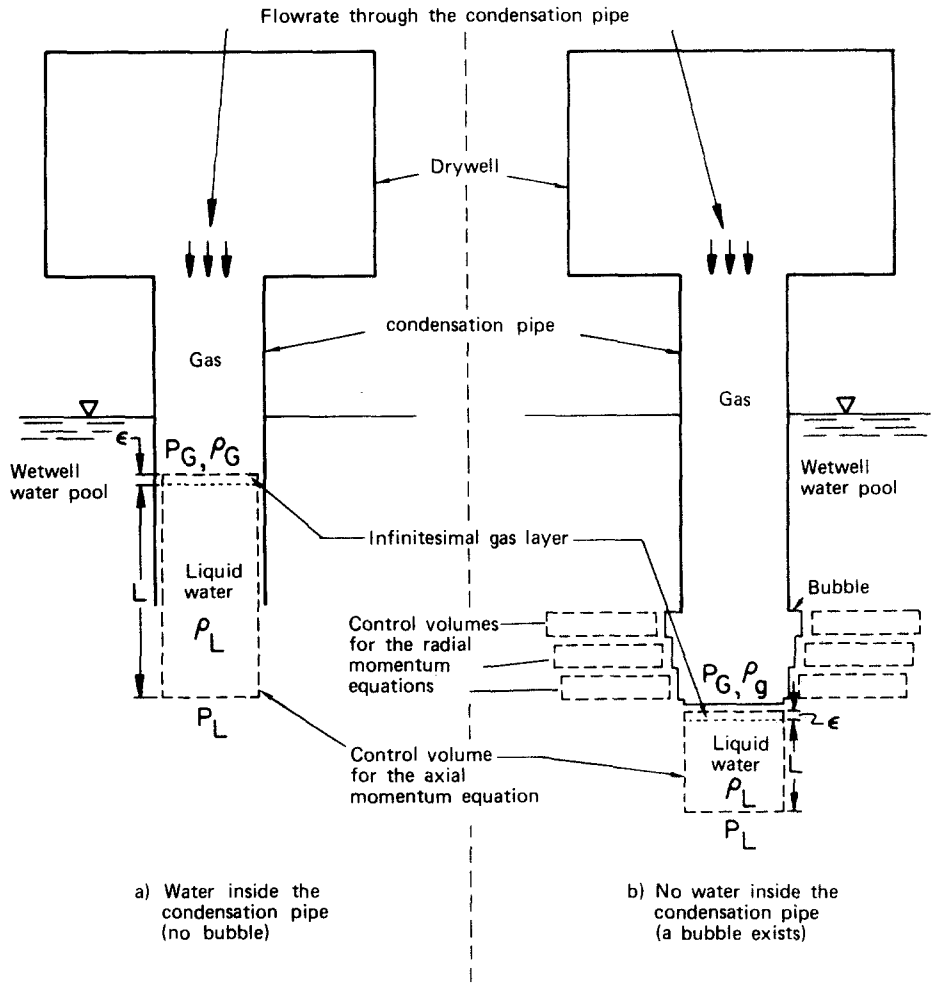

Figure 3. Calculational model for momentum transfer in the condensation pipe and the wetwell water pool.

stages of bubble collapse does the solution for the bubble shape become inaccurate. Fortunately, the time period of bubble collapse is comparatively short and the effects on the overall results are small.

The value of F_z is determined by the pressure on top of the control volume, less the pressure on the bottom, times the area of the pipe. Subtracted from this value of F_z is a term that accounts for frictional loss in the pipe and dissipation of momentum as the fluid exits from the pipe and linear motion is changed to circular vortices.

If P_G and ρ_G are the pressure and density of the gas just above the control volume; P_L and ρ_L are the pressure and density of water just below the control volume, $\lambda(L/D)$; K_i and K_0 are the frictional, and entrance and exit loss coefficients; g is the gravitational constant; A is the cross-sectional area of the condensation pipe; and ϵ is an infinitesimal gas layer in the control volumes shown in figure 3, then:

$$F_z = \begin{cases} (P_G - P_L)A - \left(\lambda\dfrac{L}{D} + K_0\right)\dfrac{\rho_L V_z^2 A}{2}, & V_z > 0 \\ (P_G - P_L)A + \left(\lambda\dfrac{L}{D} + K_i\right)\dfrac{\rho_L V_z^2 A}{2}, & V_z < 0, \end{cases} \quad [7]$$

$$\iiint_{\text{C.V.}} B_z(\rho \, dv) = g\rho_L AL, \quad [8]$$

$$\int\int_{\text{c.s.}} V_z(\rho V_z \cdot dA) = (\rho_L - \rho_G)V_z^2 A, \qquad [9]$$

$$\frac{\partial}{\partial t}\int\int\int_{\text{c.v.}} V_z(\rho\, dv) = \frac{\partial}{\partial t}\{V_z(\rho_G A\epsilon) + \rho_L AL\} = V_z^2 A(\rho_G - \rho_L) + (\rho_G\epsilon + \rho_L L)A\frac{\partial V_z}{\partial t}. \qquad [10]\dagger$$

Combining[9] and [10] in the limit when we let $\epsilon \to 0$ gives

$$\int\int_{\text{c.s.}} V_z(\rho V_z \cdot dA) + \frac{\partial}{\partial t}\int\int\int_{\text{c.v.}} V_z(\rho\, dv) = \rho_L AL\frac{\partial V_z}{\partial t}. \qquad [11]$$

The axial acceleration is found by combining [6]–[8] and [11]. Velocity and displacement are found by time integration.

When a bubble exists, as shown in figure 3(b), it is divided into nodes, the number of which is determined by dividing the distance between the bottom of the condensation pipe and the bubble bottom surface by the axial distance across each node. The number is truncated to an integer value and changes as the bubble grows or contracts. There are three nodes to the bubble shown in figure 3(b). The small region just above the bubble bottom boundary has less axial thickness than a full node and its radial boundary is not permitted to move. The radial momentum equation,

$$F_r = \int\int_{\text{c.s.}} V_r(\rho V_r \cdot dA) + \frac{\partial}{\partial t}\int\int\int_{\text{c.v.}} V_r(\rho\, dv), \qquad [12]$$

is applied to each full node and the motion of each radial control volume boundary is determined independently of its neighbors. The radial momentum equations contain no "z" direction terms and the areas now vary with radius, but otherwise they are similar to the axial momentum equation. The radial control volumes are annular disks of water whose inner radii are the surface of the bubble and whose radial thicknesses are one pipe diameter. The axial thickness of each radial control volume is equal to the node thickness.

The shape of the bubble is found by applying the axial mimentum equation to obtain the axial acceleration, then integrating over the time step to determine axial velocity and the position of the bubble bottom gas–water interface boundary. Next the radial momentum equations are applied at each active node and the resulting radial accelerations are integrated to obtain the radial bubble boundary velocities and positions.

The total amount of heat transfer consists of the sum of heat transfer through the condensation pipe side wall and at the gas–water interface. The gas–water interface can be present in the condensation pipe or it can form the surface of a bubble below the condensation pipe. Heat transfer through the side wall of the condensation pipe is determined by calculating an overall heat transfer coefficient that includes conduction through the pipe wall itself plus convection both inside and outside the condensation pipe. Convection outside the condensation pipe, modeled using natural convection on a vertical surface, was found to be the dominating factor.

The thickness of the thermal boundary layer outside the condensation pipe is approximated by laminar flow over a flat plate whose length is equal to the submergence depth of the

†In [10] it should be noted that $\frac{d\epsilon}{dt} = V_z$ and $\frac{dL}{dt} = -V_z$.

condensation pipe (Schlichting 1968). An average value is calculated which is held constant throughout the problem. The temperature in the boundary layer outside the pipe wall is set equal to the temperature of the active water pool volume (described later) when a bubble exists because the presence of the bubble generates turbulence and mixing in the water pool. This temperature increases above the active water pool volume temperature when water is inside the pipe and there is little disturbance of the active water pool. Conservation of energy within the thermal boundary layer is used to calculate this temperature increase.

When water is present in the bottom of the condensation pipe, direct contact heat transfer between steam and water is dominated either by (1) how fast heat can be transferred from the steam to the water surface, or by (2) how fast heat can be dissipated from the interface. The dominating mechanism is used to calculate the heat transfer. If (1) dominates, we must consider the insulating effects of air, which concentrates just above the interface as steam condenses there. The quantity of air is calculated from the amount of steam which condenses in a single cycle after water enters the bottom of the condensation pipe, multiplied by mass fraction of air, χ_a, present in the steam. For thin layers of air, as used in our study, heat transfer is controlled by conduction (Holman 1976). A minimum thickness of the air layer is selected as water enters the bottom of the condensation pipe so that the heat transfer coefficient is equal to 1000 kW/m^{2}K. The value of 1000 kW/m^{2}K was selected as a maximum heat transfer coefficient based on the data of Engeldinger (1977). When all water is discharged from the condensation pipe during the chugging cycle, the value of the air layer thickness is again set to its minimum value.

If turbulent diffusion dominates, the correlation documented by Kowalchuk & Sonin (1978) is used to determine the heat transfer. They consider the heat transfer coefficient, α, to be

$$\alpha = \rho_L C_L \sqrt{\left(\frac{\beta \bar{V} D}{t_1 + t}\right)}, \qquad [13]$$

with

$$t_1 = \beta \bar{V} D \left(\frac{\rho_L C_L}{a_1}\right)^2. \qquad [14]$$

Here ρ_L and C_L are the density and specific heat of water, β is an empirical coefficient equal to 0.01, $\bar{V}$ is the average mean velocity of the water inside the condensation pipe during the time water is present there, D and t are the diameter of the condensation pipe and the time, and a_1 is a minimum heat transfer coefficient obtained from Engeldinger (1977) for small bubbles. As can be seen in [13], α decreases with time.

If a bubble is present, a correlation for the heat transfer coefficient

$$\alpha = a_1 + a_2 A_b, \qquad [15]$$

is used where a_1 and a_2 are constants obtained from Engeldinger's work and A_b is the surface area of the bubble. A value of 350 kW/m^{2}K for a_1 was selected from Engeldinger's minimum value for α with small bubbles. The value of 150 kW/m^{4}K for a_2 was selected so that α is 1000 kW/m^{2}K when the bubble volume in a full-scale experiment equals that of a cylinder three pipe diameters in length. This volume is about equal to that of the large bubbles seen by Engeldinger. A value of 1000 kW/m^{2}K for α is close to the maximum reported by him.

The form of [15] is based on the fact as the bubble grows larger the actual heat transfer surface area exceeds that of a regular geometric shape because of instabilities that form. These instabilities (e.g. Taylor instabilities) create an undulating surface with hills and valleys that enhance heat transfer. Further, because of these instabilities, the value of α is not permitted to

decrease during bubble collapse, but is retained at the maximum value reached. When a new bubble is formed, α is set back to an initial value based on [15].

For calculation of heat transfer when a bubble exists or when turbulent diffusion dominates, the equation

$$Q_b = \alpha A_b \Delta T_b \qquad [16]$$

is used. Here A_b is the cross-sectional area of the condensation pipe or the surface area of the bubble, whichever is appropriate. The temperature difference between the steam and active wetwell water pool volume temperature is ΔT_b. The amount of mass flowing into the condensation pipe during a computational time step is set equal to the mass of steam condensed plus the mass of steam necessary to satisfy continuity as the water surface moves. The assumption implied is that a steady process exists. The chugging is transient in nature but the frequency in large scale facilities is less than a few hertz. This frequency is so low that accurate results can be obtained with reasonably large computational time steps using a quasi-steady state analysis.

The pressure in the wetwell air space above the water at time zero is determined by subtracting the initial static head of water from the drywell pressure. The initial static head of water is that between the water level in the wetwell and the initial water level inside the condensation pipe. The wetwell air space pressure is increased above its initial value as air from the drywell enters the wetwell. A perfect gas relationship is used, with the entering air considered to be at the temperature of the wetwell water. All steam entering the wetwell is considered to be condensed in the water pool and does not influence the increase of wetwell air-space pressure.

The volume of water in the wetwell is divided into an active portion and an inactive portion. The active portion increases in temperature with time as energy is transferred from the steam condensed in the condensation pipe and in the wetwell. Temperature in the active wetwell water pool volume is considered to be uniform. The volume is calculated as that present above the exit of the condensation pipe. It can be argued that the temperature near the condensation pipe is considerably higher than in a region far away, but above the exit, or that the volume varies with time. Experimental data (Aust 1977) indicates, however, that the assumptions incorporated here are reasonable.

Results are generated with an explicit, finite-difference computer code named SCHUG.† The main program reads the inputs; sets the material properties for air, water and steam; calculates the mass flowrate into the drywell; calls the subroutines; and indexes the time for the next iteration. The only inputs are the geometry of the problem, initial conditions and constants used to generate the mass flowrate into the drywell, and conduction heat transfer through the condensation pipe wall. The code runs rapidly with results for 500 s of real time generated in only 10 s of AMDAHL 470 computer time.

The main calculations are performed in subroutines taking known conditions at a given time, t, and calculating new conditions at a time, Δt, later. The time step, Δt, is held constant throughout the problem. All results reported here were generated with a time step of 0.01 s. Some problems, however, were run with time steps of 0.001 and 0.1 s to check the stability of the calculation. The results with the time step of 0.001 s were essentially identical to those generated with a time step of 0.01 s. This gave assurance that the results were stable.

When a time step of 0.1 s was used, results showed some variation, but this was due to lack of convergence with such a large time step rather than any difficulty with stability. No singular numbers, such as are frequently encountered with instability, were generated when a 0.1 s time step was used. A maximum time step of 2 per cent of the chugging period is permitted in SCHUG, so that convergence is assured.

†SCHUG is an acronym for Steam CHUGging

Results were found to be essentially independent of the axial length across each of the bubble nodes. Naturally, when more bubble nodes are utilized, a better definition of the bubble is obtained, and in all calculations we attempted to use at least 10 of the 20 nodes available in the computer code. However, the chugging period, pressures, etc. did not vary when as little as 5 nodes or as many as 15–20 were used.

The code can be used to predict general characteristics of chugging in existing or proposed experiments, to make parameter studies, or can be incorporated into more general codes to predict phenomena in addition to steam chugging. In conducting parameter studies, we used constant values of (1) inlet steam mass flowrate to the drywell; (2) air mass fraction in the steam; (3) wetwell water pool temperature; and (4) wetwell air space pressure. Details of the analysis and the computer code have been documented by Pitts (1979).

RESULTS

Two large scale experiments were chosen to compare with analytical results generated with SCHUG. Grosskraftwerk Mannheim (GKM) II, test number 21 (1976) was selected as the first experiment because periodic steam chugging occurred between about 60 and 160 s after the start of the test, and because records of data were available. SCHUG was then used to predict test 21. The results are shown in table 1 and in figures 4–6. The experimental chugging period, averaged over 5 chugging periods between 70 and 80 s, is shown in the table because these experimental periods varied by up to 15 per cent from the average value. The experimental value for the time a bubble exists was found by examining the trace of a thermocouple which was placed inside the condensation pipe at 0.16 pipe diameter above the exit. This trace showed a rapid increase in temperature as water passed below the thermocouple and exposed it to steam. Similarly, there was a rapid decrease in temperature as water returned inside the condensation pipe and passed above the thermocouple. A thermocouple positioned inside the condensation pipe, 5.4 diameters above the exit, exhibited no such fluctuation indicating that water never reached this point. The time that the water is inside the condensation pipe is the difference between the chugging period and the time the bubble exists.

Predicted values of the period and the other times shown in table 1 are in good agreement with these experimental values. The maximum extent of the bubble below the condensation pipe is within 30 per cent of that believed to exist when video recordings of the test are reviewed. It should be noted that the boundary of the bubble, when viewed using high speed photography, would include any surrounding mixture of liquid and vapor. Should such a mixture be present, the bubble would appear to be larger than it actually is. The predicted value of maximum bubble extent would then be even closer to experimental value. The results shown in table 1 indicate that the physics incorporated in SCHUG adequately represent the general phenomenon of steam chugging.

Table 1. Comparison of predicted and experimental times and bubble size in a single cycle

Item	SCHUG analytical model	GKM II Test 21
(1) Chugging period	2.0 s	1.9 s
Time a bubble exists	0.5 s	0.4 s
Time water is in the pipe	1.5 s	1.5 s
(2) Maximum extent of bubble below the pipe exit (in pipe diameters)	1.4	2
(3) Maximum elevation of water inside the pipe (in pipe diameters)	4	Unknown (but less then 5.4

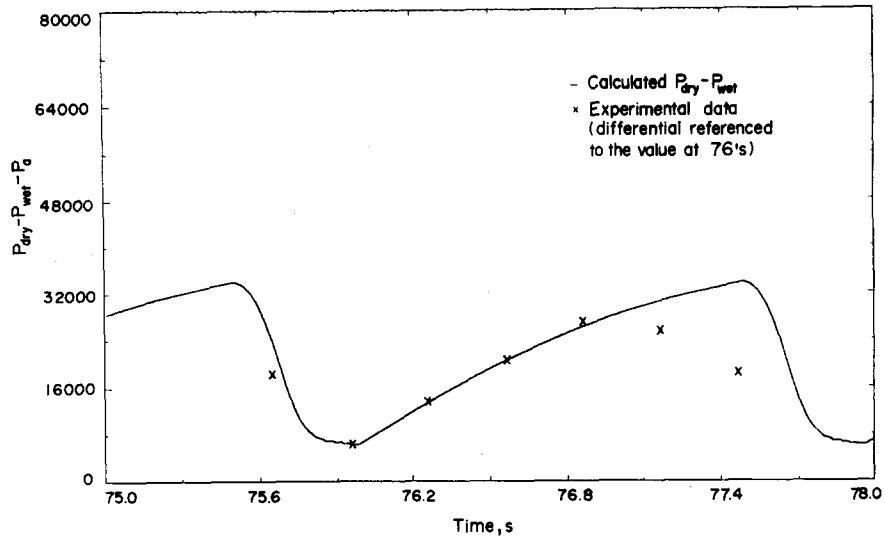

Figure 4. Comparison of calculated pressure difference between the drywell and wetwell air space with experimental data, GKM test 21.

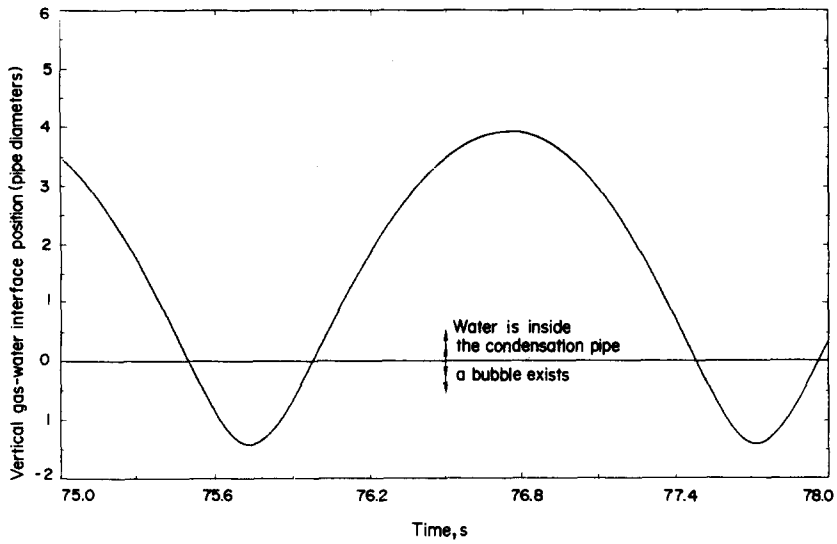

Figure 5. Predicted distance of the gas–water interface from the condensation pipe exit, GKM test 21.

Figure 4 shows the variation of the pressure difference between the drywell and the wetwell air space as a function of time. The slow rise in the curve occurs when water is present inside the pipe and the steam condensation rate is smaller than the drywell inlet steam flowrate. The more rapid drop in the curve occurs when a bubble exists and the steam condensation rate is much larger than the drywell inlet steam flowrate. Experimental data is shown by the "×" symbols. The absolute value of pressure difference could not be determined from available data. However, the magnitude of the variation in pressure difference from a reference value could be found. The reference value was taken as the minimum which occurs on the figure at 76 s. The variation in differential pressure shows close agreement with predicted values except near the far right. Here a large portion of the deviation is due to the fact that the predicted theoretical period was 7 per cent larger than the experimental period for this particular chugging cycle. If an adjustment were made for this difference between the predicted period and the experimental period, the data near the r.h.s. of the figure would be closer to the predicted curve.

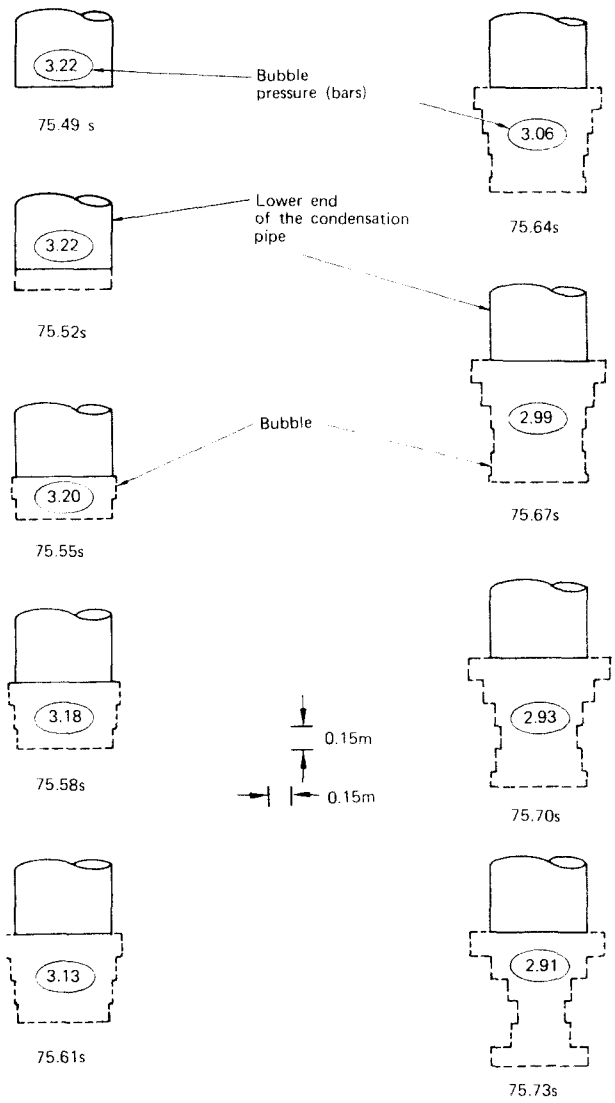

Figure 6. Predicted time variation of the bubble shape for GKM II test 21. (Circled numbers are the bubble pressure in bars.)

Figure 5 shows the vertical location of the gas–water interface with time. The ordinate is in pipe diameters with zero at the exit of the condensation pipe. A bubble exists when the interface is below zero; water is inside the condensation pipe when the interface is above zero. Note that the maximum extent of the bubble is 1.4 pipe diameters below the end of the condensation pipe, and water reaches a height 4 pipe diameters above the pipe exit.

Figure 6 shows the predicted shape of the bubble as a function of time during the period of bubble growth and start of collapse. The shape of the bubble during the later stages of bubble collapse is not included because instabilities, such as Taylor instabilities, become dominant. Note that the bubble grows in a generally cylindrical shape with a neck forming as the bubble starts to collapse. In figure 6 the numbers circled inside the bubble show the predicted pressure in bars. The pressure decreases as the bubble grows and the steam condensation rate increases.

Gesellschaft für Kernenergieverwertung in Schiffbau and Schiffahrt (GKSS) test number 16 (1977) was selected as the second experiment for comparison with analytical predictions of SCHUG for two reasons. First, the test was well documented (Aust 1977, GKSS 1978). Second, the chugging that occurred in this test was more random than that of GKM II test 21, with the bubble extending only a fraction of a pipe diameter below the exit of the condensation pipe.

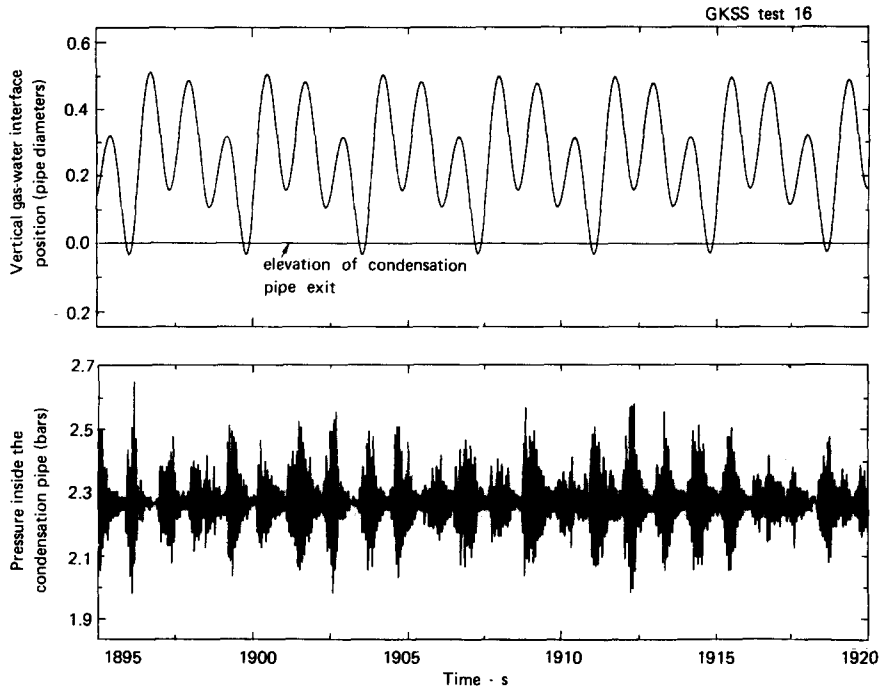

Figure 7. Comparison of predicted gas–water interface and experimental pressure oscillations.

Figure 7 can be used to compare the predicted and experimental chugging period. The location of the gas–water interface is plotted against time in the upper half of the figure. Note the the fundamental period of oscillations is about 1.25 s but that the interface leaves the condensation pipe to form a bubble only during every third cycle (negative values of the ordinate). Analytical results with SCHUG showed the fundamental period to be the same throughout the time period from 1500 to 3000 s after the start of the test but that the time between the formation of one bubble and the formation of the next bubble varied in multiples of the fundamental period.

Distinct regimes were apparent. In one regime the interface would oscillate inside the condensation pipe for two fundamental periods and in the next period it would leave the condensation pipe to form a bubble, as shown in figure 7. In another regime, the interface would oscillate for three fundamental periods inside the condensation pipe and then form a bubble in the next two fundamental periods. There were many combinations of the number of fundamental periods where the interface oscillated inside the pipe and then formed a bubble.

In general, the maximum extent of a bubble below the condensation pipe was greater at the start of a regime, then decreased until the next regime began. This change in magnitude in the maximum extent of the bubble coupled with the change from one regime to another offers a partial explanation for the apparent randomness of steam chugging observed in some experiments including GKSS test 16.

The lower portion of figure 7 shows pressure data from a transducer located inside the condensation pipe, 0.145 m above the exit. It can be observed that the fundamental period is about 1.08 s which is in good agreement with the analytical prediction of 1.25 s. The high frequency pressure oscillations present are believed to be due to the structural response of the system to the loads produced with each chug. The magnitude of the pressure oscillations varies from one fundamental period to another. This variation is an indication that sometimes a bubble could appear and at other times the interface could oscillate inside or close to the end of the condensation pipe.

A review of the GKSS test 16 videotape recording during this time period revealed that some steam was discharged from the exit of the condensation pipe during each fundamental period

but that the interface was barely below the exit. At times the videotape showed the bubble emerging up to perhaps 1/5 pipe diameter below the exit with the interface then appearing to move well inside the condensation pipe. The three-dimensional nature of the interface, which was not simulated in SCHUG, could result in some discharge of steam from the exit of the pipe even though the average position of the interface is slightly inside the condensation pipe. If this is the case, the prediction by SCHUG closely resembles the observed visual observations on the videotape.

A parameter study was next conducted with SCHUG to determine the influence of five parameters: the inlet mass flowrate into the drywell, the active wetwell water pool temperature, the fraction of air in the drywell passing through the condensation pipe with the steam, the drywell pressure, and the submergence depth of the condensation pipe exit below the wetwell water pool surface. In all cases, the input parameters were kept constant so that a steady chugging condition was obtained. Table 2 lists the nominal values and the range of parameters used in the study. The nominal parameters simulated conditions which occurred in GKSS test 16 at about 1750 s. During the study all parameters except one were kept at their nominal values. The one parameter was then varied over the range shown.

When the inlet mass flowrate into the drywell was chosen as the parameter to be varied, the gas–water interface stayed inside the condensation pipe during all problems where the flowrate was less than 0.2 kg/s. Between 0.2 and 0.8 kg/s, various regimes of chugging occurred where the interface would oscillate inside the condensation pipe a number of times and then leave the condensation pipe to form a bubble. Between 0.8 and 3.3 kg/s, the interface would oscillate once inside the condensation pipe and then move outside the condensation pipe to form a bubble. Following this, the interface would return inside for another oscillation before forming the next bubble. Figure 8 shows the maximum and minimum extent of the interface when the flowrate was between 0.8 and 3.3 kg/s. Note that as the flowrate increased, larger bubbles were formed in each cycle and the interface entered the condensation pipe to a lesser extent. Finally, above 3.3 kg/s, the interface stayed completely outside the condensation pipe and oscillations only changed the bubble size. The general characteristics were reported by Chan (1977a, b) but the values of flowrate where a certain type of chugging occurred are different. This is an indication that there may be a size effect in steam chugging not reported previously.

Variation of the active wetwell water pool temperature revealed characteristics similar to those shown during the variation of flowrate. Below 340 K, the variety of regimes of chugging occurred where the interface would oscillate inside the condensation pipe several times and then form a bubble (corresponding to 0.8–3.3 kg/s during the flowrate variation study). Between 340 and 380 K, the interface oscillated only once inside the condensation pipe before forming the next bubble. Above 380 K, the interface never entered the condensation pipe but rather oscillated outside, forming a large bubble followed by a smaller bubble.

When the air fraction in the steam passing through the condensation pipe was varied below 10^{-7}, various regimes of chugging occurred which were similar to those that occurred when the flowrate was varied between 0.8 and 3.3 kg/s. Above a value of air fraction equal to 10^{-5}, the chugging occurred at a period of 1.2 s with the interface extending inside the condensation pipe about 0.3 m and then forming a bubble with maximum extent of about 0.15 m before returning inside the condensation pipe. Variation of the air fraction above 10^{-5} had little effect on the

Table 2. Parameters used in the GKSS test 16 parameter study

Parameter	Nominal value	Range of variation
(1) Inlet steam mass flowrate into the drywell	0.60 kg/s	0.05–6.0 kg/s
(2) Wetwell water pool temperature	333.5 K	310–390 K
(3) Fraction of air in the drywell	7×10^{-14}	10^{-50}–0.10
(4) Drywell pressure	2.19×10^5 Pa	1.0×10^5–5.0×10^5 Pa
(5) Condensation pipe submergence	3.802 m	1.0–8.0 m

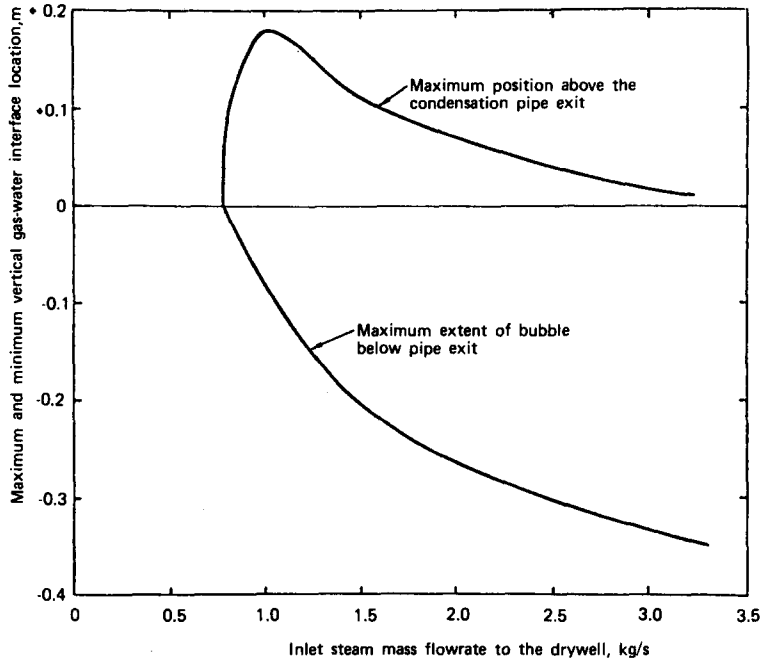

Figure 8. Effect of steam mass flowrate on maximum and minimum vertical gas–water interface location.

chugging characteristics. The influence of air fractions of such small magnitudes is surprising. This may be due to the assumed uniform thickness of the air layer above the gas–water interface when water is present inside the condensation pipe. Turbulence and the three-dimensional nature of this air layer would reduce its insulating properties so that larger air fractions would be needed to obtain the same effects.

Variation of the drywell pressure or the submergence of the condensation pipe resulted in changes in the regimes of chugging (similar to a flowrate variation betwen 0.8 and 3.3 kg/s), but in all cases the interface oscillated several times inside the condensation pipe before forming a bubble. Effects of drywell pressure and pipe submergence on the results appear to be reasonable small.

CONCLUSIONS

(1) A transient analysis, based on physical principles, was developed to predict general characteristics of steam chugging. No arbitrary free parameters, which must be specified to predict specific experiments, are present. Results of the analysis are in agreement with two large scale tests. The naalysis may be used to preduct general characteristics of steam chugging in nuclear power plants or experimental tests, and can be incorporated into larger general computer programs or used as part of a BWR pressure–suppression system fluid-structure analysis.

(2) The apparent randomness of steam chugging observed in some experiments (including GKSS test 16) may be due, in part, to the appearance of different regimes of chugging. In one regime the gas–water interface may oscillate inside the condensation pipe for several cycles before emerging to form a bubble. In another regime, the interface may oscillate for only one cycle before forming a bubble. Coupled with changes in the maximum extent of a bubble below the condensation pipe exit during each chugging regime, the formation of a bubble appears to be somewhat random.

(3) A parameter study indicates a dependency of chugging on the steam inlet mass flowrate into the drywell, the wetwell active water pool temperature, and the air fraction contained in

the steam passing through the condensation pipe. Chugging appears to be less sensitive to changes in drywell pressure and condensation pipe submergence.

Acknowledgements—This research was supported by the Ministers for Research and Technology in the Federal Republic of Germany under the framework of RS 263/6, and by the Dept. of Energy in the U.S. under Contract W-7405-ENG-48.

REFERENCES

ANDEEN, G. B. & MARKS, J. S. 1979 Analysis and testing of steam chugging in pressure systems. SRI International report prepared for the Electric Power Research Institute, EPRI NP-908.

AUST, E., FÜRST, D., NIEMANN, H.-R., SCHWAN, H. & VOLLBRANDT, J. 1977 & 1978 Druckabbauversuche auf dem PSS-Versuchsstand der GKSS-Ergebnisse des versuchs Nr. 16 (1. Hauptversuche). Versuchtsbericht Nr. 73 03 AR E 16. Gesellschaft für Kernenergieverwertung in Schiffbau and Schiffahrt mbH, Geesthacht, Federal Republic of Germany, Rep. GKSS 77/I/24; similar documents for tests 17–21, Reps. GKSS 77/I/33, 77/I/38, 77/I/42 and 78/I/2.

CHAN, C. K. *et al.* 1977a Studies of dynamic loads in pressure suppression containment. Quarterly reports from July to September and October to December 1977. U.S. Nuclear Regulatory Commission Reps. NUREG/CR-0039 and NUREG/CR-0067.

CHAN, C. K. *et al.* 1977b Suppression pool dynamics. Annual report, U.S. Nuclear Regulatory Commission Rep. NUREG-0264-3.

CHAN, C. K., DHIR, V. K. & LIU, C. Y. 1978 Studies of dynamic loads in pressure suppression containment. Quarterly report, January–March 1978, prepared for the U.S. Nuclear Regulatory Commission by the Chemical, Nuclear and Thermal Engng Dept. of the University of California, LA.

CLASS, G. 1977 Theoretische untersuchung der druckpulsentwicklung bei der dampkondensation im druckabbausystem von siedewasserreaktoren-rechenprogramm KONDAS. Kernforschungszentrum Karlsruhe, Federal Republic of Germany, Rep. KFK 2487.

ENGELDINGER, M. 1977 Diplomarbeit—Untersuchung der Kondensation von Sattdampf in einer Wasservorlage anhand von Hochgeschwindigkeitsfilmaufnahmen. Universität Karlsruhe (TH), Institut für Reaktortechnik, in particular figures 15 and 16.

Gesellschaft fur Kernenergieverwertung in Schiffbau and Schiffahrt (GKSS) mbH, Federal Republic of Germany 1978 Erste experimentelle Ergebnisse zur Dampfkondensation am Kondensationsrohr mit Einschnürung. Rep. 73 03 AR B 46.

Grosskraftwerk Mannheim (GKM) II test 21, Federal Republic of Germany, 1976.

HOLMAN, J. P. 1976 *Heat Transfer*, 4th Edn, p. 256. McGraw-Hill, New York.

KOCH, E. & KARWAT, H. 1976 Research efforts in the area of BWR pressure-suppression experiments. *4th Water Reactor Safety Research Information Meeting*, Gaithersburg, Maryland, November 1976,

KOWALCHUK, W. & SONIN, A. A. 1978 A model for condensation oscillations in a vertical pipe discharging steam into a subcooled water pool. U.S. Nuclear Regulatory Commission Rep. NUREG/CR-0221.

Marviken Power Station, Sweden The Marviken full scale containment experiments. Containment reponse to a loss of coolant accident—summary report, Rep. MXA-1-301.

PITTS, J. H. 1979 Analysis of boiling-water reactor steam chugging, Gesellschaft für Reaktorsicherheit (GRS) mbH, 8046 Garching, Federal Republic of Germany, Rep. GKS-A-259.

SARGIS, D. A., STUHMILLER, J. H. & WANG, S. S. 1979 Analysis of steam chugging phenomena. Jaycor report prepared for the Electric Power Research Institute, EPRI NP-908.

SCHLICHTING, H. 1968 *Boundary-Layer Theory*, 6th Edn, pp. 130 and 265. McGraw-Hill, New York.

SHAMES, I. H. 1962 *Mechanics of Fluids*, Chap. 5. McGraw-Hill, New York.